Published in final edited form as:
Development. 2005 November ; 132(22): 5055–5068. doi:10.1242/dev.02088.

Mice deficient in Ext2 lack heparan sulfate and develop exostoses

Dominique Stickens[1,*], **Beverly M. Zak**[2,†], **Nathalie Rougier**[1,†,‡], **Jeffrey D. Esko**[2], and **Zena Werb**[1,§]

[1]Department of Anatomy, University of California, San Francisco, CA 94143-0452, USA

[2]Department of Cellular and Molecular Medicine, Biomedical Sciences Graduate Program, University of California, San Diego, La Jolla, CA 92093-0687, USA

Summary

Hereditary multiple exostoses (HME) is a genetically heterogeneous human disease characterized by the development of bony outgrowths near the ends of long bones. HME results from mutations in *EXT1* and *EXT2*, genes that encode glycosyltransferases that synthesize heparan sulfate chains. To study the relationship of the disease to mutations in these genes, we generated *Ext2*-null mice by gene targeting. Homozygous mutant embryos developed normally until embryonic day 6.0, when they became growth arrested and failed to gastrulate, pointing to the early essential role for heparan sulfate in developing embryos. Heterozygotes had a normal lifespan and were fertile; however, analysis of their skeletons showed that about one-third of the animals formed one or more ectopic bone growths (exostoses). Significantly, all of the mice showed multiple abnormalities in cartilage differentiation, including disorganization of chondrocytes in long bones and premature hypertrophy in costochondral cartilage. These changes were not attributable to a defect in hedgehog signaling, suggesting that they arise from deficiencies in other heparan sulfate-dependent pathways. The finding that haploinsufficiency triggers abnormal cartilage differentiation gives insight into the complex molecular mechanisms underlying the development of exostoses.

Keywords

Homologous recombination; Knockout; Hypertrophic cartilage; Chondrocyte; Hereditary multiple exostoses; Heparan sulfate; Mouse

Introduction

Heparan sulfate proteoglycans (HSPG) are present in the extracellular matrix and on the surface of virtually every cell type. They consist of a core protein to which heparan sulfate is covalently attached. In vitro, HS interacts with a multitude of molecules, including growth factors and extracellular matrix proteins. Much of our knowledge about the in vivo function of HS in extracellular signaling cascades stems from studies in *Drosophila* (Lin, 2004). However, in recent years, analyses of targeted mutations in animals and human disorders caused by mutations in HS production have vastly increased our understanding of the in vivo role of HS

§Author for correspondence (zena@itsa.ucsf.edu).
*Present address: Merck Research Laboratories, 126 Lincoln Avenue, Rahway, NJ 07065-0900, USA
†These authors contributed equally to this work
‡Present address: Hôpital Bichat–Claude-Bernard, 46 Rue Henri-Huchard, 75018 Paris, France

Supplementary material Supplementary material for this article is available at http://dev.biologists.org/cgi/content/full/132/22/5055/DC1

in development and disease (for reviews see Esko and Selleck, 2002; Nakato and Kimata, 2002).

Hereditary multiple exostoses (HME) is a skeletal disorder characterized by the presence of multiple bony protuberances called exostoses (or osteochondromas), usually arising in the epiphyseal growth plate of bones formed by endochondral ossification. Although exostoses can be found on almost every long bone, they appear more frequently at the distal end of the femur, tibia, fibula, humerus and ribs. Often, the formation of an exostosis interferes with normal bone development, resulting in deformities such as shortening and bowing of the bones (Hennekam, 1991; Solomon, 1963). HME is a multigenic disease and follows an autosomal dominant mode of inheritance. Approximately 80% of affected individuals have a positive family history, although exostoses can also appear sporadically. Genetic linkage studies and mutation analyses have identified two main loci as being associated with the disease: *EXT1*, located on chromosome 8q24.1; and *EXT2*, located on chromosome 11p11 (Ahn et al., 1995; Stickens et al., 1996).

HS is a glycosaminoglycan (GAG), a linear polysaccharide composed of alternating D-glucuronic acid (GlcA) and *N*-acetyl-D-glucosamine (GlcNAc) subunits. The biosynthesis of HS is a complex process that involves a whole host of enzymes (for review see Esko and Selleck, 2002). The *EXT1* and *EXT2* genes encode the exostosins, glycosyltransferases involved in the synthesis of HS (Lind et al., 1998; McCormick et al., 1998; Wei et al., 2000). EXT1 and EXT2 are type II transmembrane proteins involved in HS chain elongation, catalyzing the alternating transfer of GlcA and GlcNAc residues. In vivo, EXT1 and EXT2 form a hetero-oligomeric complex in the Golgi apparatus and this complex has a higher glycosyltransferase activity than either protein alone (McCormick et al., 2000; Senay et al., 2000). The majority of cases of HME are caused by frameshift or missense mutations in EXT1 or EXT2, creating truncated forms of the proteins they encode (Ahn et al., 1995; Stickens et al., 1996; Wuyts and Van Hul, 2000; Zak et al., 2002). The clinical syndromes of HME caused by mutations at the *EXT1* or the *EXT2* loci are identical, and no phenotype-genotype correlations exist (Cook et al., 1993; Le Merrer et al., 1994; Wu et al., 1994).

The initial identification of EXT genes as glycosyltransferases did not yield an immediate understanding of the biological processes they control. If HS is present on almost every cell type, then why do mutations in EXT genes lead primarily to a bone phenotype? Further insight into the function of EXT genes was obtained through the identification of the *Drosophila* Ext genes *tout-velu* (homolog of EXT1), *sister of tout-velu* (homolog of EXT2) and *brother of tout-velu* (homolog of EXTL3) (Bellaiche et al., 1998; Han et al., 2004; Takei et al., 2004). Mutations in these genes result in the accumulation of Hedgehog, Wingless and Decapentaplegic proteins in front of the mutant cells, suggesting that HS is required for generating morphogen gradients. This was an important finding, as mutations in EXT genes affect bone formation, and all three morphogens [Hedgehog, Wnt proteins and bone morphogenic proteins (BMPs)] have a role in skeletal development (Karsenty and Wagner, 2002).

Targeted deletion of *Ext1* in mice results in early embryonic lethality and *Ext1*-null embryos die around the time of gastrulation. Inactivation of Ext1 abolishes the production of HS, illustrating the importance of Ext genes in HS synthesis (Lin et al., 2000). *Ext1* heterozygous mice show somewhat increased chondrocyte proliferation and delayed hypertrophic differentiation owing to increased Indian hedgehog [Ihh (Hilton et al., 2005)], but are not reported to show any gross skeletal phenotype. Other evidence of a direct relationship between Ihh, Ext genes and bone development has come from the analysis of mice with a hypomorphic *Ext1* allele ($Ext1^{gt/gt}$) that was generated by a gene-trap method (Koziel et al., 2004). In contrast to *Ext1*-null mice, $Ext1^{gt/gt}$ mice survive until E14.5 and some embryos can be recovered at

E16.5. Interestingly, in the growth plates of *Ext1*$^{gt/gt}$ mice, Ihh has an expanded range of signaling. These data suggest that Ext1 might play a role in endochondral ossification by modulating the distribution of Ihh. As EXT1 and EXT2 form a complex and HME is caused by mutations in either gene, we generated mice deficient for *Ext2* and analyzed the homozygous and heterozygous phenotypes to better understand the etiology of this disease.

Materials and methods

Construction of the targeting vector

A 12 kb genomic clone was obtained by screening a 129Sv mouse genomic library (Stratagene) with a probe derived from the 5′ end of the mouse *Ext2* cDNA. A 2.1 kb *Xho*I-*Bst*EII fragment from intron 1 was cloned upstream of a neomycin-resistance (Neo) gene and downstream of a thymidine kinase (TK) gene to form the 5′ vector arm. The neo and TK genes are under control of the phosphoglycerokinase (PGK) promoter and the herpes simplex virus (HSV) promoter, respectively. The 3′ vector arm was created by cloning a 3.5 kb *Not*I-*Hin*dIII fragment downstream of the neo gene. The targeting vector was linearized by digestion with *Not*I and electroporated into ES cells. After 10 days of treatment with G418 (Geneticin, 180 μg/ml Invitrogen) and FIAU [1(-2-deoxy-2-fluoro-b-D-arabinofuranosyl)-S-iodouracil] for positive-negative selection, respectively, ES colonies were picked and tested for homologous recombination. Selected clones were karyotyped to test for chromosomal abnormalities. Three independent heterozygous ES clones were injected into C57BL/6 blastocysts to generate chimeric mice. A total of seven chimeric animals were produced, two of which transmitted the mutation through the germline. Mice heterozygous for the *Ext2* mutant allele gave rise to litters of normal size when bred to wild-type animals.

Genotyping

ES cell DNA and mouse tail DNA were screened for the *Ext2* targeted mutation by digestion with *Spe*I or *Hin*dIII, followed by southern blot hybridization with probe A or probe B, respectively (see Fig. S1 in the supplementary material). Replacement of exon 2 of the *Ext2* gene with a neo cassette introduced *Spe*I and *Hin*dIII sites that could be used to distinguish the wild-type allele from the targeted allele. Upon digestion of genomic DNA with *Spe*I and hybridization with probe A, wild-type and targeted alleles produced fragments of 9 kb and 5.3 kb, respectively. Following digestion with *Hin*dIII and hybridization with probe B, wild-type and targeted alleles produced fragments of 6 kb and 3.5 kb, respectively. Probe A is a 1.8 kb *Spe*I-*Hin*dIII fragment external to the region of vector homology. Probe B is a 300 bp PCR amplification product (forward primer, 5′ACATTATGATCACATATTGC; reverse primer, 5′ GGAGTACAATGAACTGCTGACG3′), 3′ from exon2 and internal to the region of vector homology. PCR genotyping was accomplished using a four-primer PCR amplification (wild-type allele: Ext2-GT-150F, GGTCTGGACGATAGGTGTCAGG; Ext2-GT-640F, GTGACGTAGTAGATTCGGTGC; the amplification product is 190 bp) (targeted allele: Ext2-GT-810R, GTTGAACAATCCAATCCACGC; Ext2-GT-NEO-R, CATGCTCCAGACTGCCTTGG; the amplification product is 260 bp).

Trophoblast stem cells (TSC)

TSC were isolated as previously described (Tanaka et al., 1998) with some modifications: 3.5 dpc mouse blastocysts were isolated from *Ext2*$^{+/-}$ C57BL/6 mice crossings. They were individually plated into four-well plates and cultured on mouse embryonic fibroblasts (MEF) in MEF medium + Fgf4 (25 ng/ml) + heparin (1 μg/ml). The medium was changed on day 3 and the blastocyst outgrowths were trypsinized on day 4 or 5. Flat colonies appeared between day 6 and day 10 and were split once they had reached 50% confluence. The medium was changed every 2 days and the cells were passaged at 80 to 90% confluence at 1 part in 10 or 20. When the blastocyst outgrowths or the cell lines were trypsinized, the doses of Fgf4 and

heparin used for the cultures were 1.5× the normal dose. TSC were weaned from the MEFs after two passages.

Histological analyses and immunohistochemistry

Tissues were fixed in 4% paraformaldehyde in phosphate-buffered saline, decalcified in EDTA, paraffin embedded, sectioned at 5 μm and stained with von Kossa's stain, Safranin O/Fast Green or Masson Trichrome. Briefly, for Safranin O/Fast Green staining, deparaffinized rehydrated sections were stained in Weigert's Iron Hematoxylin (Sigma,), 0.02% aqueous Fast Green (Sigma) followed by a rinse in 1% acetic acid and 0.1% aqueous Safranin O (Sigma). For Masson Trichrome staining, a kit was used according to the instructions of the manufacturer (Sigma).

For immunohistochemistry, tissues were fixed, embedded and sectioned as described above. For HS immunostaining, sections were deparaffinized, washed in PBS and any endogenous peroxidase activity was blocked using 0.3% hydrogen peroxide (Sigma) in methanol for 30 minutes at ambient temperature. Sections were rinsed in PBS and incubated with M.O.M. blocking solution (M.O.M. kit, Vector Laboratories) for 1 hour at room temperature. After rinsing in PBS, sections were incubated overnight at 4°C with the mouse monoclonal antibody 10E4 (Seikagaku) at a dilution of 1:100. Unbound antibody was removed by washing in PBS. Bound antibody was detected using an HRP-conjugated anti-mouse IgM secondary antibody (Jackson ImmunoResearch Laboratories) for 1 hour at ambient temperature. After washing in PBS, the peroxidase was detected using a DAB detection kit (Zymed). Sections were washed in tap water and counterstained with Methyl Green (Sigma). Control sections were overlaid with 2.5 mU of heparitinase I (Sigma) in 0.5 ml of buffer (100 mM NaCl, 1 mM $CaCl_2$, 50 mM sodium HEPES, pH 7.0, containing 25 mg of BSA) for 2 hours at 37°C. After rinsing in PBS, sections were incubated with the HS antibody 10E4 as described above.

Preparation and staining of whole skeletons

Whole skeletal preparations of 2-week-old mice were prepared and stained with Alizarin Red and Alcian Blue as previously described (McLeod, 1980). For the measurements of bone length and localization of exostoses, skeletons were prepared by Dermestid beetles as described (Hefti et al., 1980).

BrdU labeling and histology

A 10 mg/ml stock of bromodeoxyuridine (BrdU; Sigma) was injected intraperitoneally into one-week-old mice at a dose of 100 μg BrdU/g. Mice were sacrificed 1 hour after injection, bones were harvested and processed as described in the section 'Histological analyses and immunohistochemistry'. Staining for BrdU was carried out on paraffin sections using a kit according to manufacturer's directions (Zymed).

RT-PCR analysis

Poly (A) RNA was isolated (Micro-FastTrack, Invitrogen) from TSC according to manufacturer instructions. cDNA was synthesized using a kit from Invitrogen (Two-step RT-PCR system) and used as template for PCR reactions using the following primers: Ext2-exon2 forward, 5′ GTGGATGATGCCGGTGTTCC 3′; Ext2-exon3 reverse, 5′ CAGGCAACATATTGAACAGC 3′; Ext2-exon8 forward, 5′ CCTACAGATCATCAATGACAGG 3′; Ext2-exon9 reverse, 5′ AGCAGCTTGGACAGACTGG 3′. Primer sets represent coding regions that span introns. E-cadherin primers were used as a control for RNA integrity. PCR amplification was performed using 30 cycles and products were analyzed on 2% agarose gels.

In situ hybridization

Paraffin sections were placed on acid-etched, TESPA-treated slides and prepared for in situ hybridization as described (Albrecht et al., 1997). Plasmids were linearized with the appropriate restriction enzymes to transcribe either sense or antisense ^{35}S-labeled riboprobes. Probes were as follows: collagen type 2 (*Col2a1*), collagen type 10 (*col10a)*, Indian hedgehog (*Ihh*) and patched 1 (*Ptch1*) (Albrecht et al., 1997; Ferguson et al., 1999); parathyroid hormone/parathyroid hormone-like peptide receptor (*Pthr1*) (Kobayashi et al., 2002); *Fgf8* (Crossley and Martin, 1995); brachyury (Wilkinson et al., 1990); *Apoe* (Basheeruddin et al., 1987); *H19* (Poirier et al., 1991); *Lim1* (Shawlot and Behringer, 1995); *Snai1* (Nieto et al., 1992); *Otx2* (Simeone et al., 1993); and *Hesx1* (Thomas and Beddington, 1996). Slides were washed at a final stringency of 65°C in 23×SSC, dipped in emulsion and exposed for 1-2 weeks. Slides were counterstained with Hoechst 33342 or Hematoxylin.

Protein purification, immunoprecipitation and western blotting

Cell culture supernatants (with or without serum) were collected on ice in the presence of protease inhibitors [pepstatin (5 μg/ml), leupeptin (1 μg/ml), aprotinin (10 μg/ml), benzamidine (10 μg/ml) (Sigma)], centrifuged at 150 ***g*** for five minutes at 4°C to remove non-adherent cells and cell debris, aliquoted and stored at −80°C. Whole-cell lysates were prepared by scraping cultured cells into RIPA buffer (20 mM Tris pH 7.2, 10 mM EDTA, 0.3 M NaCl, 0.1% SDS, 1% Triton X100, 0.05% Tween 20) containing the same protease inhibitors. Cell debris was removed by centrifugation at 20,000 ***g*** for 20 minutes at 4°C and the protein aliquots were stored at −80°C until used. The BCA protein assay kit (Pierce, Rockford, IL) was used to determine the protein concentration of the supernatants and of the cell lysates. The polyclonal antibody against Ext2 was a generous gift from Dr Takahiko Shimizu (Tokyo Metropolitan Institute of Gerontology) (Morimoto et al., 2002).

Analyses of glycosaminoglycan chains and cellular enzyme activities

Trophoblast stem cells or ES cells were cultured for 72 hours in a medium composed of 70% MEF-conditioned medium and 30% sulfate-depleted RPMI medium or for 48 hours with 50 μCi/ml of $^{35}SO_4$ (Dupont NEN) in sulfate-reduced F12 medium, respectively. [^{35}S]GAG chains were isolated by DEAE chromatography and a sample was treated with chondroitinase ABC at 37°C overnight (Bame and Esko, 1989). Treated and untreated chains were separated by anion-exchange HPLC. Glycosaminoglycans were eluted with a linear gradient of NaCl (0.2-1 M) using a flow rate of 1 ml/minute and increasing the NaCl concentration by 10 mM/minute. The effluent from the column was monitored for radioactivity with an in-line radioactivity detector (Radiomatic floOne/beta, Packard Instruments) with sampling rates every 6 seconds and data averaged over 1-minute intervals.

Results

Inactivation of Ext2 results in defective heparan sulfate synthesis

To better understand the function of the *Ext2* gene, we inactivated it through homologous recombination in ES cells. A targeting vector was constructed in which a neomycin-resistance cassette replaced exon 2, which contains the start of translation (see Fig. S1 in the supplementary material). Three independent Ext2 heterozygous ES clones were injected into C57BL/6 blastocysts and chimeric mice were mated with wild-type C57BL/6 to generate germline mutant mice.

We expected that inactivation of Ext2 would also abolish HS synthesis. To test this hypothesis, we isolated wild type, *Ext2*$^{+/-}$ and *Ext2*$^{-/-}$ TSC, and collected RNA for RT-PCR analyses (Fig. 1A). As expected, no amplification product was obtained in an RT-PCR reaction using primers

for exon 2. However, an amplification product of the expected size was obtained when primers for exon 8 were used, indicating that a truncated form of the Ext2 RNA transcript was being made. Cell lysates from wild-type, heterozygous and *Ext2*$^{-/-}$ TSC were analyzed by western blot (Fig. 1B). Incubation with a polyclonal antibody against EXT2 showed an expected band of 82 kDa in cell lysates from wild-type and *Ext2*$^{+/-}$ TSC. However, heterozygotes showed a second band of lower molecular weight and of varying intensity, suggesting that a truncated form of the protein was being produced. Immunoblots of lysates from Ext2$^{-/-}$ cells revealed that these cells express only the truncated form of the protein.

ES cells derived from wild-type, heterozygous and null embryos were grown in culture with $^{35}SO_4$ to label sulfated glycosaminoglycans, which in wild-type cells consist of a mixture of HS and chondroitin sulfate (CS) (Lin et al., 2000). A sample of the ^{35}S-GAG chains was analyzed by anion exchange chromatography directly and another sample was first treated with chondroitinase ABC, which depolymerizes chondroitin sulfate. As shown in Fig. 1C, wild-type and heterozygous Ext2 ES cells both produced two peaks of labeled material. The first peak was resistant to chondroitinase and signifies HS, whereas the second peak was sensitive to chondroitinase and signifies CS. *Ext2*$^{-/-}$ ES cells only produced one peak, which co-eluted with CS and was sensitive to chondroitinase, and thus no HS was being produced.

Next, we verified that HS was not produced by staining sections of E7.5 wild-type and Ext2$^{-/-}$ embryos with an antibody that recognizes HS (10E4) (Fig. 1D). In wild-type embryos, a strong signal was detected in the basement membranes of the ectodermal, endodermal and mesodermal cell layers. By contrast, specific staining for HS was not detected in *Ext2*$^{-/-}$ mutants. Therefore, although an immunoreactive fragment of the Ext2 protein is produced, it is inactive in HS synthesis.

Loss of Ext2 results in early embryonic lethality

Mice heterozygous for the *Ext2* mutant allele appeared phenotypically normal and gave rise to litters of normal size when crossed with wild-type animals. We did not detect any *Ext2*$^{-/-}$ neonates from nearly 300 offspring of *Ext2* heterozygous intercross matings, indicating that mutant mice died during embryogenesis (Table 1). To characterize the embryonic lethality, timed *Ext2*$^{+/-}$ matings were set up and embryos were genotyped and morphologies examined starting at E6.0. At E6.0, Ext2 mutants were indistinguishable from wild-type embryos (data not shown). However, at E6.5 the first visible and reproducible differences with wild-type embryos became apparent (Fig. 2A,B). Mutant embryos appeared to have formed a normal ectoplacental cone, but the extra-embryonic regions were underdeveloped and the egg cylinder did not elongate. At E7.5, all wild-type embryos had initiated gastrulation and had formed a primitive streak. Although all of the mutants were smaller than wild-type embryos, there was heterogeneity with respect to the degree of egg cylinder elongation and formation of extra-embryonic structures connecting the embryonic structures to the ectoplacental cone (Fig. 2C,D). Despite the morphological variation of *Ext2*$^{-/-}$ embryos, none of the mutants showed any visible evidence of primitive streak formation (Fig. 2E-H). By E8.5, the *Ext2*$^{-/-}$ embryos had degenerated and lacked recognizable structures (data not shown).

Ext2$^{-/-}$ embryos initiate primitive streak formation but fail to form mesoderm

We examined the mutants in greater detail in order to determine the precise stages of development impacted by the lack of HS. At E7.5, control embryos had developed a primitive streak and mesodermal cells were visible between the ectoderm and visceral endoderm. At this stage, we observed three different classes of morphologically distinct *Ext2*$^{-/-}$ mutants (Fig. 2F-H). In all three types of mutants, parietal endoderm and Reichert's membrane had elongated to almost the same size as the wild-type embryo. However, no histologically recognizable primitive streak or mesoderm (embryonic or extra-embryonic) formed in any of the mutants.

The first group (class 1) represented about 25% of all mutants and was characterized by a round-shaped egg cylinder that appeared to be directly connected to the ectoplacental cone (Fig. 2F). No extra-embryonic ectoderm, endoderm or mesoderm was present. The egg cylinder consisted of only two layers, ectoderm and visceral endoderm, with no primitive streak or mesoderm. The cells of the ectodermal layer were pycnotic and TUNEL assays confirmed a significant increase in the number of apoptotic cells in this layer (Fig. 2J). We excluded class 1 embryos from further analyses as they were no longer viable.

A second class of mutants (class 2), representing about 50% of all mutants, developed some extra-embryonic structures, but they were composed of immature extra-embryonic ectoderm and endoderm, when compared with wild type, and lacked extra-embryonic mesoderm entirely (Fig. 2G). The egg cylinder had elongated to about one-third the size of the wild-type embryos, but only consisted of embryonic ectoderm and visceral endoderm. TUNEL assays showed only a few apoptotic cells (Fig. 2K).

A third group of Ext2 mutants (class 3), showed further elongation of the embryonic and extra-embryonic regions, but still no embryonic or extra-embryonic mesoderm was present (Fig. 2H). Interestingly, these mutants had initiated the formation of a head fold and histological analyses showed the presence of neuroectoderm. This region of the embryo contained a high number of TUNEL-positive cells (Fig. 2L). Further histological analyses indicated that cavitation was taking place in the region of TUNEL-positive cells (data not shown).

H19, a marker for extra-embryonic tissues (Poirier et al., 1991), was expressed in $Ext2^{-/-}$ embryos and confirmed that extra-embryonic ectoderm and endoderm, and ectoplacental cone and trophoblast giant cells were present and not significantly affected (Fig. 3A,B). Apolipoprotein E (*Apoe*), a marker for visceral endoderm (Basheeruddin et al., 1987), was expressed in $Ext2^{-/-}$ embryos, indicating that Ext2 is not required for ectoderm or endoderm formation (Fig. 3C,D). Interestingly, expression of Fgf8, one of the earliest markers for primitive streak formation (Crossley and Martin, 1995; Maruoka et al., 1998), was detected in wild-type embryos as well as in *Ext2* mutants, albeit at reduced levels (Fig. 3E,F). However, as *Fgf8* is normally expressed just prior to streak formation in a patch of epiblast cells on the proximal prospective posterior side, ands in the visceral endoderm (Crossley and Martin, 1995), this expression does not necessarily indicate that Ext2 mutants are capable of forming a primitive streak. By contrast, another marker of the primitive streak and mesodermal cells, brachyury (T) (Wilkinson et al., 1990), was present in wild-type embryos, but not in Ext2 mutants at E6.5 (Fig. 3G,H).

Both class 2 (Fig. 3I,J) and class 3 (Fig. 3K,L) mutants expressed *T* at E7.5. At the midstreak stage, *Lim1* mRNA is expressed at low levels in the primitive streak and at higher levels in mesodermal cells migrating away from the streak. By E7.5, its expression is restricted to the node (Barnes et al., 1994). In $Ext2^{-/-}$ class 3 mutants, we found several cells expressing *Lim1* in the region where the primitive streak would normally form (Fig. 3O,P). However, *Snai1*, which is expressed in cell populations that will become migratory, including primitive streak and nascent mesoderm (Nieto et al., 1992; Smith et al., 1992), was not expressed in $Ext2^{-/-}$ embryos (Fig. 3Q,R). These results suggest that $Ext2^{-/-}$ embryos initiate the formation of a primitive streak, but fail to properly form mesoderm.

Our histological analyses indicated that some E7.5 $Ext2^{-/-}$ embryos can initiate the formation of a head fold and accumulate neuroectoderm. *Otx2* is normally detected in anterior neuroectoderm at late streak stage, in the region encompassing the prospective forebrain and midbrain (Ang et al., 1994; Simeone et al., 1993). *Hesx1* is initially expressed in anterior visceral endoderm (AVE) and subsequently in definitive endoderm. *Hesx1* expression then intensifies and spreads laterally into neuroectoderm, but remains restricted to the most anterior

region of the brain (Hermesz et al., 1996; Thomas and Beddington, 1996). Therefore, we performed in situ hybridization with *Otx2* and *Hesx1* probes, and were able to confirm that the anterior cell mass observed in the $Ext2^{-/-}$ mutants is indeed neuroectoderm (Fig. 3S,T).

Ext2 heterozygous mice form exostoses

Humans with HME are heterozygous for either EXT1 or EXT2. Close examination of the skeletons of $Ext2^{+/-}$ mice revealed the presence of one or more exostoses on the ribs of 7 out of 25 (28%) Ext2 heterozygotes, whereas exostoses were never detected in wild-type animals (Fig. 4A,B). In humans, ribs are a common location for exostoses formation, although nearly every bone, with the exception of membranous bones, is involved. However, we did not find exostoses on the long bones (tibia, femur, ulna and radius) of the $Ext2^{+/-}$ mice. Despite this difference, the exostoses we examined in the mice were very similar to those seen in humans and varied in shape and size from a small widening of the metaphyseal region to a large bulky outgrowth. Most mice only had a single exostosis (range 1-3). The distribution of lesions was uniform throughout the rib cage and there was no preferential orientation of the projection (ventrally, dorsally or laterally).

Mouse exostoses resembled those in humans. The lesions were located near the costochondral junction and were composed of cortical and medullary bone with an overlying hyaline cartilage cap (Fig. 4C-E). Characteristic for exostoses, the bone marrow cavity was continuous with that of the underlying bone. The cartilage cap was covered with a thin layer of fibrous tissue that was continuous with the perichondrium. Within the cartilage cap we found random patches of calcification. Some chondrocytes appeared to be lined up, resembling the organization of chondrocytes in a normal growth plate. Histological sections of the exostosis cartilage cap stained positive for HS with the HS antibody 10E4 (Fig. 4F). These results demonstrate that chondrocytes of the exostosis produce HS, and are therefore not null for *Ext2*.

Frequently, the formation of exostoses is accompanied by short stature (Hennekam, 1991). It has been previously reported that $Ext1^{+/-}$ mice have a ~10% reduction in bone length (Lin et al., 2000). We examined bone length in $Ext2^{+/-}$ mice on the C57BL/6 background. Skeletons at 12 weeks of age were cleaned by Dermestid beetles and found no significant difference in either total length [wild type, 95.2±0.534 mm (n=27); $Ext2^{+/-}$, 96.0±0.637 mm (n=25); P=0.351, two-tailed t-test], measured from tip of the snout to base of the tail, or in the ratio of total length divided by length of tibia plus femur [wild type, 2.90±0.012 mm (n=25); $Ext2^{+/-}$, 2.91±0.014 mm (n=25); P=0.887, two-tailed t-test). Our re-evaluation of $Ext1^{+/-}$ mice also showed no significant differences in bone length (B.M.Z., D.S., M. Hilton, G. Evans, Z.W., D. Wells and J.D.E., unpublished).

Ribs of $Ext2^{+/-}$ mice show chondrocyte abnormalities

We also observed a 100% penetrant phenotype in postnatal Ext2 heterozygotes: nodules or single misplaced chondrocytes were detected on every rib and appeared throughout the entire length of the costochondral cartilage (Fig. 5A). These displaced chondrocytes were present as single cells (Fig. 5B) or as clusters (Fig. 5C) near the perichondrium. On rare occasions, a nodule was large enough to be detected on a whole-mount skeletal stain (Fig. 5D). The abnormal chondrocytes were always found with overlying perichondrium. In many cases, this appeared to make the perichondrium bulge out.

Interestingly, these chondrocyte abnormalities seen in the $Ext2^{+/-}$ mice, between 1 and 2 weeks of age, occur at the same time the rib cartilage undergoes hypertrophic differentiation. Before 1 week of age, chondrocytes in the ribs of wild-type mice have a uniform undifferentiated appearance throughout the costochondral cartilage (Fig. 6A,B; also see Fig. 10). Around 2 weeks of age, however, chondrocytes in the center of the skeletal element mature and become

hypertrophic, while cells in the periphery remain small and undifferentiated. In situ hybridization confirmed that the morphological changes correspond to changes in expression of differentiation-specific genes. Up to 1 week of age, all chondrocytes express Col2, an early marker of chondrocyte differentiation (Fig. 6C,D). At 2 weeks of age, expression of Col2 is restricted to cells at the periphery (Fig. 6E,F). Chondrocytes in the center now express Col10, a marker of hypertrophic chondrocytes (Fig. 6G).

This raises the issue of whether the formation of the nodules was the result of a defect in proliferation and/or differentiation. Older animals tended to have nodules that were bigger, suggesting that nodules could result from clonal expansion of one or more displaced chondrocytes (compare Fig. 5B,C). When we injected BrdU into 2-week-old *Ext2*$^{+/-}$ mice and collected ribs 1 hour later, we found BrdU-positive cells in the proliferative zone of the growth plate of the ribs, as expected (Fig. 7A-C). There were no BrdU-positive cells in any other region of the costochondral cartilage where the nodules form or in the nodules themselves of the *Ext2*$^{+/-}$ ribs. The nodules, therefore, did not appear to be highly proliferative.

As the displaced cartilage had the appearance of prematurely differentiated chondrocytes, we performed in situ hybridization analysis with a Col10 antisense probe to check for evidence of cartilage hypertrophy (Fig. 7D). At 2 weeks of age, hypertrophic cells in the center of the rib cartilage expressed Col10, while cells in the periphery did not. The nodules of displaced chondrocytes expressed Col10, but were separated from the centrally located hypertrophic cells by a layer of chondrocytes that did not express Col10. This thin layer of cells did express Col2 (data not shown). These data indicate that cells in the nodule had differentiated prematurely. Staining with the HS antibody 10E4 further showed that the chondrocytes in the nodules still produced HS, and thus were not *Ext2*$^{-/-}$ cells (Fig. 7E).

We next asked what mechanism underlies these defects in cartilage formation. The Ihh/Pthr1 pathway was a good candidate, as altered activation of this pathway can potentiate chondrocyte differentiation. We observed that, although Ihh is expressed in the growth plate of rib cartilage at the time the defects appear, it is absent from the rest of the rib cartilage and from areas where premature differentiation was observed (data not shown). To determine hedgehog activity more sensitively, we crossed the *Ext2*$^{+/-}$ mice with mice carrying *lacZ* under control of the hedgehog receptor patched 1 (Ptch1). At 1-2 weeks of age, when the premature hypertrophic differentiation was observed, no *lacZ* staining could be found in the rib cartilage other than in the growth plate of the rib (data not shown; see Fig. 10 for schematic representation of expression domains). This result is in agreement with our in situ analysis and indicates that there is no aberrant hedgehog activity in the *Ext2*$^{+/-}$ chondrocytes.

What is the mechanism of cartilage hypertrophy? *Pthlp*$^{-/-}$ mice show hypertrophic differentiation that is reversed by introducing a constitutively active Pthr1 under the control of the Col2 promoter (Soegiarto et al., 2001). To test whether the abnormal chondrocyte hypertrophy seen in the nodules of the *Ext2*$^{+/-}$ ribs was due to reduced Pthlp signaling, we crossed the constitutively active Col2-Pthr1 transgene into the *Ext2*$^{+/-}$ mice (Fig. 8). However, this was unable to prevent the premature hypertrophic differentiation of the rib cartilage of *Ext2*$^{+/-}$ mice. Taken together, these data suggest that the rib cartilage abnormalities seen in the *Ext2*$^{+/-}$ mice are not the direct result of alterations in Ihh/ Pthr1 signaling.

Ext2$^{+/-}$ mice show chondrocyte abnormalities in growth plates of long bones

The phenotype seen in the ribs prompted us to look for phenotypes in the growth plates of long bones. There were no overt morphological differences in growth plates in histological sections of ulna, radius and femur from E18.5 wild-type and *Ext2*$^{+/-}$ mice (Fig. 9A,B). Mineralization of the cartilage matrix, formation of the bony collar surrounding the hypertrophic chondrocytes and formation of trabecular bone all appeared to be normal (Fig. 9E,F).

To assess chondrocyte proliferation, we injected pregnant females with bromodeoxyuridine (BrdU) and embryos collected at E18.5. We found no significance in the overall number of BrdU-positive cells (wild type 33.1±2.5, n=12; $Ext2^{+/-}$ 34.4±2.0, n=11; P=0.70, unpaired t-test) in the proliferating zone of the growth plate (Fig. 9G,H).

However, closer examination of the chondrocytes in the proliferative zone showed a loss of the characteristic columnar organization normally seen in wild-type growth plates (Fig. 9A-D). Although the organizational defect in $Ext2^{+/-}$ long bones was subtle, it was consistent for all (8/8) bones examined. Similar chondrocyte disorganization was observed in embryonic mice homozygous for a gene trap insertion in the *Ext1* gene ($Ext1^{gt/gt}$) (Koziel et al., 2004).

In wild-type mice, *Pthr1* and *Ihh* are expressed in prehypertrophic chondrocytes in domains that were partially overlapping (Fig. 9K,L and Fig. 9M,N, respectively). *Ptch1* was expressed in the perichondrium, adjacent to the expression domain of *Ihh* and in proliferating chondrocytes (Fig. 9I,J). $Ext2^{+/-}$ mice expressed *Ptch1*, *Ihh* and *Pthr1* in the appropriate places, but there was a small decrease in the expression domains of *Pthr1* and *Ihh*, while the *Ptch1* expression domain in $Ext2^{+/-}$ seemed comparable with that in wild type. We then analyzed the distribution of Ihh protein by immunohistochemistry using Ab80, a sonic hedgehog antibody that crossreacts with Ihh. We did not see any obvious difference in the localization of the hedgehog protein between wild type and $Ext2^{+/-}$ (data not shown). These data show that inactivation of one allele of Ext2 interferes with normal chondrocyte development. However, as we could not detect any differences in total length of bones, this differentiation defect does not appear to influence the endochondral ossification process in any significant way.

Discussion

Ext1 and Ext2 are glycosyltransferases involved in the chain elongation of heparan sulfate (Lind et al., 1998; McCormick et al., 2000; Wei et al., 2000). Prior studies of Ext1 in mice demonstrated that this gene is essential for HS synthesis and early development (Lin et al., 2000). We have shown for the first time that the expression of Ext2 is essential for HS synthesis in mice, confirming studies in *Drosophila* (Bornemann et al., 2004; Takei et al., 2004) and zebrafish (Lee et al., 2004).

Lack of mesoderm formation in *Ext2*-null mutants

Inactivation of Ext2 results in early embryonic lethality around the time of gastrulation. The morphogenic movements and differentiation of cells that accompany gastrulation are in large part directed by signaling molecules, such as members of the transforming growth factorβ (Tgfβ) superfamily (Zhao, 2003), Wnt proteins (Kelly et al., 2004) and Fgf proteins (Ciruna and Rossant, 2001). Many of these signaling molecules can bind HS, at least in vitro (for a review, see Lin, 2004). Our data show that inactivation of Ext2 abolishes production of HS, possibly resulting in an effect on one or more of these signaling pathways. One candidate is Ihh, as mice with a gene trap mutation in the Ext1 gene have altered Indian hedgehog signaling (Koziel et al., 2004). However, *Ihh*-null mutants die around mid-gestation, between 10.5 and 12.5 dpc (St-Jacques et al., 1999), much later than the *Ext2*-null mice.

The lack of Ext2 leads to a gastrulation defect and abnormalities in the formation of extra-embryonic structures. As proteoglycans are required for gastrulation and specifically to promote Fgf signaling (Garcia-Garcia and Anderson, 2003), it is plausible that FGF signaling is affected in Ext mutants. However, *Fgf4* and *Fgfr2* mutant mice die shortly after implantation (Arman et al., 1998; Feldman et al., 1995), and thus have an earlier phenotype than Ext-null mice. Ext mutants share some similarities with *Fgfr1* and *Fgf8* mutants, although they differ greatly with respect to formation of extra-embryonic structures.

The lack of properly organized extra-embryonic structures and lack of mesoderm are more reminiscent of defects caused by mutations in members of the TGFβ-superfamily. Bmp4 is required for formation of the extra-embryonic mesoderm and epiblast cell proliferation (Winnier et al., 1995), while Nodal plays a role in primitive streak formation (Conlon et al., 1994). Although inactivation of Wnt3a affects gastrulation (Yoshikawa et al., 1997), *Wnt3a*-null embryos have a defect that is less severe than that of *Ext1* or *Ext2* mutants. It seems more likely that the defects observed in the Ext mutants are the result of alterations in multiple signaling pathways.

Exostoses formation and chondrocytes differentiation abnormalities

HME is characterized by the presence of multiple bony outgrowths or lumps on the metaphyses of long bones. In this study, we show that exostoses formed in Ext2 heterozygote mice with all of the features found in human exostoses. To determine why exostoses in mice only form on the ribs is in principle no different from asking why individuals with HME do not have exostoses on all of their bones. Is there a phenotype that is common to all heterozygotes that could predispose them to exostoses formation? Indeed, we found a subtle disorganization of late proliferative chondrocytes in the growth plates of all bones of the *Ext2* heterozygotes and a small but reproducible decrease in the expression zone of Ihh and Pthr1. However, Ihh expression was greatly reduced postnatally and, thus, it is possible that there was a difference in diffusion of the Ihh protein, too subtle to be detected with our methods. Alternatively, the disorganization of chondrocytes could be the result of changes in the ECM caused by the reduction of HS.

Between 1 and 2 weeks of age, cells in the center of the rib cartilage become hypertrophic and express Col10, while cells in the periphery remain less differentiated and continue to express Col2. The mechanisms that control this differentiation process have not been fully elucidated; however, it has been demonstrated that in the long bones, Ihh and Pthlh signaling are required for proper chondrocyte differentiation. The premature hypertrophic differentiation seen in the $Ext2^{+/-}$ mice suggests that the Ihh/Pthr1 pathway might be involved; however, our observations do not support this idea.

The *EXT1* and *EXT2* genes have been suggested to function as tumor suppressor genes on the basis of studies showing loss of heterozygosity for markers around the *EXT1* and *EXT2* loci in both sporadic and exostosis-derived chondrosarcomas (Hecht et al., 1995). Our analyses show a reduction in the amount of HS in the chondrocyte zones of exostoses, but never a total loss, lending further support to the model that exostoses formation is the result of haploinsufficiency.

The dependence of FGF signaling pathways on HS has been well documented. In the long bones, FGF signaling shortens proliferative columns both by decreasing chondrocyte proliferation directly and by suppressing Ihh expression (Minina et al., 2002; Naski and Ornitz, 1998; Ornitz and Marie, 2002). Bmps antagonize the effects of Fgf signaling (Minina et al., 2002; Minina et al., 2001). Mutations in *Ext1* and *Ext2* decrease HS synthesis, which might result in reduced Fgf signaling, leading to defects in chondrocyte differentiation. Our preliminary data support the hypothesis that altered Fgf signaling could cause the Ext2 phenotype (B.M.Z., D.S., M. Hilton, G. Evans, Z.W., D. Wells and J.D.E., unpublished).

An intriguing issue is whether the premature differentiation of chondrocytes leads to the formation of exostoses or whether distinct processes cause the two phenomena. It has been suggested that the formation of the exostoses is the result of a defect in the bony collar that surrounds the growth plate. Alternatively, the passage of the growth plate might result in vascularization of the tissue, causing the chondrocytes in the nodule, which have an opposite orientation of differentiation, to initiate the outgrowth of an exostosis at a 90° angle from the parent bone (Fig. 10). During rib growth, the ratio of cartilage to bone in the ribs is essentially

constant. The probability of the growth plate passing a nodule is relatively small, as the nodules appear only between 1 and 2 weeks, and are rare compared with the overall number of chondrocytes. Thus, the random distribution of nodules relative to the growth plate could explain the low penetrance and variable distribution of exostoses.

Supplementary Material

Refer to Web version on PubMed Central for supplementary material.

Acknowledgments

We thank Doris Brown for all the help in creating the *Ext2* knockout mice and Ernestina Schipani for providing the constitutively active Pthr1 mice. We are grateful to Helen Capili for her outstanding patience and skill in sectioning the many skeletal elements. We thank Takahiko Shimizu for his generous donation of the EXT2 polyclonal antibody and Denise Piscopo for reading and discussing the manuscript. This work was supported by funds from the National Institutes of Health (AR46238 and AG23218 to Z.W. and GM33063 to J.D.E.). D.S. was a Wyeth fellow of the Life Sciences Research Foundation. B.M.Z. was supported by a minority supplement to grant GM33063.

References

Ahn J, Ludecke HJ, Lindow S, Horton WA, Lee B, Wagner MJ, Horsthemke B, Wells DE. Cloning of the putative tumour suppressor gene for hereditary multiple exostoses (EXT1). Nat. Genet 1995;11:137–143. [PubMed: 7550340]

Albrecht, U.; Eichele, G.; Helms, JA.; Lu, H. Visualization of gene expression patterns by in situ hybridization. In: Daston, G., editor. Molecular and Cellular Methods in Developmental Toxicology. CRC Press; Boca Raton: 1997. p. 23-48.

Ang SL, Conlon RA, Jin O, Rossant J. Positive and negative signals from mesoderm regulate the expression of mouse Otx2 in ectoderm explants. Development 1994;120:2979–2989. [PubMed: 7607086]

Arman E, Haffner-Krausz R, Chen Y, Heath JK, Lonai P. Targeted disruption of fibroblast growth factor (FGF) receptor 2 suggests a role for FGF signaling in pregastrulation mammalian development. Proc. Natl. Acad. Sci. USA 1998;95:5082–5087. [PubMed: 9560232]

Bame KJ, Esko JD. Undersulfated heparan sulfate in a Chinese hamster ovary cell mutant defective in heparan sulfate N-sulfotransferase. J. Biol. Chem 1989;264:8059–8065. [PubMed: 2524478]

Barnes JD, Crosby JL, Jones CM, Wright CV, Hogan BL. Embryonic expression of Lim-1, the mouse homolog of Xenopus Xlim-1, suggests a role in lateral mesoderm differentiation and neurogenesis. Dev. Biol 1994;161:168–178. [PubMed: 7904966]

Basheeruddin K, Stein P, Strickland S, Williams DL. Expression of the murine apolipoprotein E gene is coupled to the differentiated state of F9 embryonal carcinoma cells. Proc. Natl. Acad. Sci. USA 1987;84:709–713. [PubMed: 3468509]

Bellaiche Y, The I, Perrimon N. Tout-velu is a Drosophila homologue of the putative tumour suppressor EXT-1 and is needed for Hh diffusion. Nature 1998;394:85–88. [PubMed: 9665133]

Bornemann DJ, Duncan JE, Staatz W, Selleck S, Warrior R. Abrogation of heparan sulfate synthesis in Drosophila disrupts the Wingless, Hedgehog and Decapentaplegic signaling pathways. Development 2004;131:1927–1938. [PubMed: 15056609]

Ciruna B, Rossant J. FGF signaling regulates mesoderm cell fate specification and morphogenetic movement at the primitive streak. Dev. Cell 2001;1:37–49. [PubMed: 11703922]

Conlon FL, Lyons KM, Takaesu N, Barth KS, Kispert A, Herrmann B, Robertson EJ. A primary requirement for nodal in the formation and maintenance of the primitive streak in the mouse. Development 1994;120:1919–1928. [PubMed: 7924997]

Cook A, Raskind W, Blanton SH, Pauli RM, Gregg RG, Francomano CA, Puffenberger E, Conrad EU, Schmale G, Schellenberg G, et al. Genetic heterogeneity in families with hereditary multiple exostoses. Am. J. Hum. Genet 1993;53:71–79. [PubMed: 8317501]

Crossley PH, Martin GR. The mouse Fgf8 gene encodes a family of polypeptides and is expressed in regions that direct outgrowth and patterning in the developing embryo. Development 1995;121:439–451. [PubMed: 7768185]

Esko JD, Selleck SB. Order out of chaos: assembly of ligand binding sites in heparan sulfate. Annu. Rev. Biochem 2002;71:435–471. [PubMed: 12045103]

Feldman B, Poueymirou W, Papaioannou VE, DeChiara TM, Goldfarb M. Requirement of FGF-4 for postimplantation mouse development. Science 1995;267:246–249. [PubMed: 7809630]

Ferguson C, Alpern E, Miclau T, Helms JA. Does adult fracture repair recapitulate embryonic skeletal formation? Mech. Dev 1999;87:57–66. [PubMed: 10495271]

Garcia-Garcia MJ, Anderson KV. Essential role of glycosaminoglycans in Fgf signaling during mouse gastrulation. Cell 2003;114:727–737. [PubMed: 14505572]

Han C, Belenkaya TY, Khodoun M, Tauchi M, Lin X. Distinct and collaborative roles of Drosophila EXT family proteins in morphogen signalling and gradient formation. Development 2004;131:1563–1575. [PubMed: 14998928]

Hecht JT, Hogue D, Strong LC, Hansen MF, Blanton SH, Wagner M. Hereditary multiple exostosis and chondrosarcoma: linkage to chromosome II and loss of heterozygosity for EXT-linked markers on chromosomes II and 8. Am. J. Hum. Genet 1995;56:1125–1131. [PubMed: 7726168]

Hefti E, Trechsel U, Rufenacht H, Fleisch H. Use of dermestid beetles for cleaning bones. Calcif. Tissue Int 1980;31:45–47. [PubMed: 6770972]

Hennekam RCM. Hereditary multiple exostosis. J. Med. Genet 1991;28:262–266. [PubMed: 1856833]

Hermesz E, Mackem S, Mahon KA. Rpx: a novel anterior-restricted homeobox gene progressively activated in the prechordal plate, anterior neural plate and Rathke's pouch of the mouse embryo. Development 1996;122:41–52. [PubMed: 8565852]

Hilton MJ, Gutierrez L, Martinez DA, Wells DE. EXT1 regulates chondrocyte proliferation and differentiation during endochondral bone development. Bone 2005;36:379–386. [PubMed: 15777636]

Karsenty G, Wagner EF. Reaching a genetic and molecular understanding of skeletal development. Dev. Cell 2002;2:389–406. [PubMed: 11970890]

Kelly OG, Pinson KI, Skarnes WC. The Wnt co-receptors Lrp5 and Lrp6 are essential for gastrulation in mice. Development 2004;131:2803–2815. [PubMed: 15142971]

Kobayashi T, Chung UI, Schipani E, Starbuck M, Karsenty G, Katagiri T, Goad DL, Lanske B, Kronenberg HM. PTHrP and Indian hedgehog control differentiation of growth plate chondrocytes at multiple steps. Development 2002;129:2977–2986. [PubMed: 12050144]

Koziel L, Kunath M, Kelly OG, Vortkamp A. Ext1-dependent heparan sulfate regulates the range of Ihh signaling during endochondral ossification. Dev. Cell 2004;6:801–813. [PubMed: 15177029]

Le Merrer M, Legeai-Mallet L, Jeannin PM, Horsthemke B, Schinzel A, Plauchu H, Toutain A, Achard F, Munnich A, Maroteaux P. A gene for hereditary multiple exostoses maps to chromosome 19p. Hum. Mol. Genet 1994;3:717–722. [PubMed: 8081357]

Lee JS, von der Hardt S, Rusch MA, Stringer SE, Stickney HL, Talbot WS, Geisler R, Nusslein-Volhard C, Selleck SB, Chien CB, et al. Axon sorting in the optic tract requires HSPG synthesis by ext2 (dackel) and extl3 (boxer). Neuron 2004;44:947–960. [PubMed: 15603738]

Lin X. Functions of heparan sulfate proteoglycans in cell signaling during development. Development 2004;131:6009–6021. [PubMed: 15563523]

Lin X, Wei G, Shi Z, Dryer L, Esko JD, Wells DE, Matzuk MM. Disruption of gastrulation and heparan sulfate biosynthesis in EXT1-deficient mice. Dev. Biol 2000;224:299–311. [PubMed: 10926768]

Lind T, Tufaro F, McCormick C, Lindahl U, Lidholt K. The putative tumor suppressors EXT1 and EXT2 are glycosyltransferases required for the biosynthesis of heparan sulfate. J. Biol. Chem 1998;273:26265–26268. [PubMed: 9756849]

Maruoka Y, Ohbayashi N, Hoshikawa M, Itoh N, Hogan BL, Furuta Y. Comparison of the expression of three highly related genes, Fgf8, Fgf17 and Fgf18, in the mouse embryo. Mech. Dev 1998;74:175–177. [PubMed: 9651520]

McCormick C, Leduc Y, Martindale D, Mattison K, Esford LE, Dyer AP, Tufaro F. The putative tumour suppressor EXT1 alters the expression of cell-surface heparan sulfate. Nat. Genet 1998;19:158–161. [PubMed: 9620772]

McCormick C, Duncan G, Goutsos KT, Tufaro F. The putative tumor suppressors EXT1 and EXT2 form a stable complex that accumulates in the Golgi apparatus and catalyzes the synthesis of heparan sulfate. Proc. Natl. Acad. Sci. USA 2000;97:668–673. [PubMed: 10639137]

McLeod MJ. Differential staining of cartilage and bone in whole mouse fetuses by alcian blue and alizarin red S. Teratology 1980;22:299–301. [PubMed: 6165088]

Minina E, Wenzel HM, Kreschel C, Karp S, Gaffield W, McMahon AP, Vortkamp A. BMP and Ihh/PTHrP signaling interact to coordinate chondrocyte proliferation and differentiation. Development 2001;128:4523–4534. [PubMed: 11714677]

Minina E, Kreschel C, Naski MC, Ornitz DM, Vortkamp A. Interaction of FGF, Ihh/Pthlh, and BMP signaling integrates chondrocyte proliferation and hypertrophic differentiation. Dev. Cell 2002;3:439–449. [PubMed: 12361605]

Morimoto K, Shimizu T, Furukawa K, Morio H, Kurosawa H, Shirasawa T. Transgenic expression of the EXT2 gene in developing chondrocytes enhances the synthesis of heparan sulfate and bone formation in mice. Biochem. Biophys. Res. Commun 2002;292:999–1009. [PubMed: 11944914]

Nakato H, Kimata K. Heparan sulfate fine structure and specificity of proteoglycan functions. Biochim. Biophys. Acta 2002;1573:312–318. [PubMed: 12417413]

Naski MC, Ornitz DM. FGF signaling in skeletal development. Front. Biosci 1998;3:D781–D794. [PubMed: 9683641]

Nieto MA, Bennett MF, Sargent MG, Wilkinson DG. Cloning and developmental expression of Sna, a murine homologue of the Drosophila snail gene. Development 1992;116:227–237. [PubMed: 1483390]

Ornitz DM, Marie PJ. FGF signaling pathways in endochondral and intramembranous bone development and human genetic disease. Genes Dev 2002;16:1446–1465. [PubMed: 12080084]

Poirier F, Chan CT, Timmons PM, Robertson EJ, Evans MJ, Rigby PW. The murine H19 gene is activated during embryonic stem cell differentiation in vitro and at the time of implantation in the developing embryo. Development 1991;113:1105–1114. [PubMed: 1811930]

Senay C, Lind T, Muguruma K, Tone Y, Kitagawa H, Sugahara K, Lidholt K, Lindahl U, Kusche-Gullberg M. The EXT1/EXT2 tumor suppressors: catalytic activities and role in heparan sulfate biosynthesis. EMBO Rep 2000;1:282–286. [PubMed: 11256613]

Shawlot W, Behringer RR. Requirement for Lim1 in head-organizer function. Nature 1995;374:425–430. [PubMed: 7700351]

Simeone A, Acampora D, Mallamaci A, Stornaiuolo A, D'Apice MR, Nigro V, Boncinelli E. A vertebrate gene related to orthodenticle contains a homeodomain of the bicoid class and demarcates anterior neuroectoderm in the gastrulating mouse embryo. EMBO J 1993;12:2735–2747. [PubMed: 8101484]

Smith DE, del Amo F. Franco, Gridley T. Isolation of Sna, a mouse gene homologous to the Drosophila genes snail and escargot: its expression pattern suggests multiple roles during postimplantation development. Development 1992;116:1033–1039. [PubMed: 1295727]

Soegiarto DW, Kiachopoulos S, Schipani E, Juppner H, Erben RG, Lanske B. Partial rescue of PTH/PTHrP receptor knockout mice by targeted expression of the Jansen transgene. Endocrinology 2001;142:5303–5310. [PubMed: 11713230]

Solomon L. Hereditary multiple exostosis. J. Bone Joint Surg 1963;45:292–304.

St-Jacques B, Hammerschmidt M, McMahon AP. Indian hedgehog signaling regulates proliferation and differentiation of chondrocytes and is essential for bone formation. Genes Dev 1999;13:2072–2086. [PubMed: 10465785]

Stickens D, Clines G, Burbee D, Ramos P, Thomas S, Hogue D, Hecht JT, Lovett M, Evans GA. The EXT2 multiple exostoses gene defines a family of putative tumour suppressor genes. Nat. Genet 1996;14:25–32. [PubMed: 8782816]

Takei Y, Ozawa Y, Sato M, Watanabe A, Tabata T. Three Drosophila EXT genes shape morphogen gradients through synthesis of heparan sulfate proteoglycans. Development 2004;131:73–82. [PubMed: 14645127]

Tanaka S, Kunath T, Hadjantonakis AK, Nagy A, Rossant J. Promotion of trophoblast stem cell proliferation by FGF4. Science 1998;282:2072–2075. [PubMed: 9851926]

Thomas P, Beddington R. Anterior primitive endoderm may be responsible for patterning the anterior neural plate in the mouse embryo. Curr. Biol 1996;6:1487–1496. [PubMed: 8939602]

Wei G, Bai X, Gabb MM, Bame KJ, Koshy TI, Spear PG, Esko JD. Location of the glucuronosyltransferase domain in the heparan sulfate copolymerase EXT1 by analysis of Chinese hamster ovary cell mutants. J. Biol. Chem 2000;275:27733–27740. [PubMed: 10864928]

Wilkinson DG, Bhatt S, Herrmann BG. Expression pattern of the mouse T gene and its role in mesoderm formation. Nature 1990;343:657–659. [PubMed: 1689462]

Winnier G, Blessing M, Labosky PA, Hogan BL. Bone morphogenetic protein-4 is required for mesoderm formation and patterning in the mouse. Genes Dev 1995;9:2105–2116. [PubMed: 7657163]

Wu Y, Heutink P, De Vries BBA, Sandkuijl LA, Van den Ouweland AMW, Niermeijer MF, Galjaard H, Reyniers E, Willems PJ, Halley DJJ. Assignment of a second locus for multiple exostoses to the pericentromeric region of chromosome 11. Hum. Mol. Genet 1994;3:167–171. [PubMed: 8162019]

Wuyts W, Van Hul W. Molecular basis of multiple exostoses: mutations in the EXT1 and EXT2 genes. Hum. Mutat 2000;15:220–227. [PubMed: 10679937]

Yoshikawa Y, Fujimori T, McMahon AP, Takada S. Evidence that absence of Wnt-3a signaling promotes neuralization instead of paraxial mesoderm development in the mouse. Dev. Biol 1997;183:234–242. [PubMed: 9126297]

Zak BM, Crawford BE, Esko JD. Hereditary multiple exostoses and heparan sulfate polymerization. Biochim. Biophys. Acta 2002;1573:346–355. [PubMed: 12417417]

Zhao GQ. Consequences of knocking out BMP signaling in the mouse. Genesis 2003;35:43–56. [PubMed: 12481298]

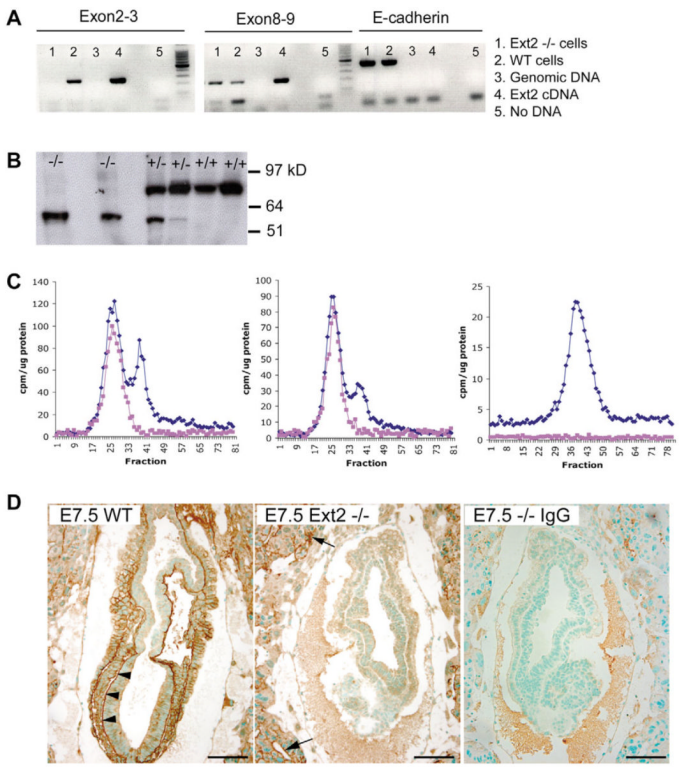

Fig. 1.

Analyses of heparan sulfate synthesis. (A) RT-PCR analyses of wild-type and *Ext2*$^{+/-}$ trophoblast stem cells (TSC). RT-PCR using a forward primer for exon 2 and a reverse primer for exon 3 shows a band of the correct size in the control lanes (2 and 4). No band can be detected in the lane with DNA from *Ext2*$^{-/-}$ TSC. When a forward primer against exon 8 and a reverse primer against exon 9 were used, a band in the lane with DNA from *Ext2*$^{-/-}$ TSC (4) is visible. Amplification with primers for E-cadherin was used as a control. (B) Western blot analyses. Cell lysates from wild-type, *Ext2*$^{+/-}$ and *Ext2*$^{-/-}$ TSC were incubated with a polyclonal antibody against EXT2 and show expected bands of 82 kDa in cell lysates from wild-type and *Ext2*$^{+/-}$ TSC. Lysates from *Ext2*$^{+/-}$ TSC show a second band of lower molecular weight. The lysates from *Ext2*$^{-/-}$ TSC show only the lower molecular weight protein. (C) ES cells derived from wild-type (left), *Ext2*$^{+/-}$ (middle) and *Ext2*$^{-/-}$ (right) embryos were grown in culture with $35SO_4$ and their GAGs were isolated. The blue symbols represent the recovery of counts before chondroitinase digestion, whereas the red points represent the recovery of counts after chondroitinase ABC digestion. *Ext2*$^{-/-}$ cells did not produce HS. (D) 10E4, an antibody that recognizes HS was used on sections of E7.5 wild-type (left) and *Ext2*$^{-/-}$ (middle) embryos. There is strong staining in the basement membranes of the wild-type embryo (arrowheads). Staining for HS was greatly diminished in *Ext2*$^{-/-}$ mutants, but strong staining can be seen in the maternal deciduae (arrows). The right-hand image shows incubation with IgG as a negative control. Scale bars: 100 μm.

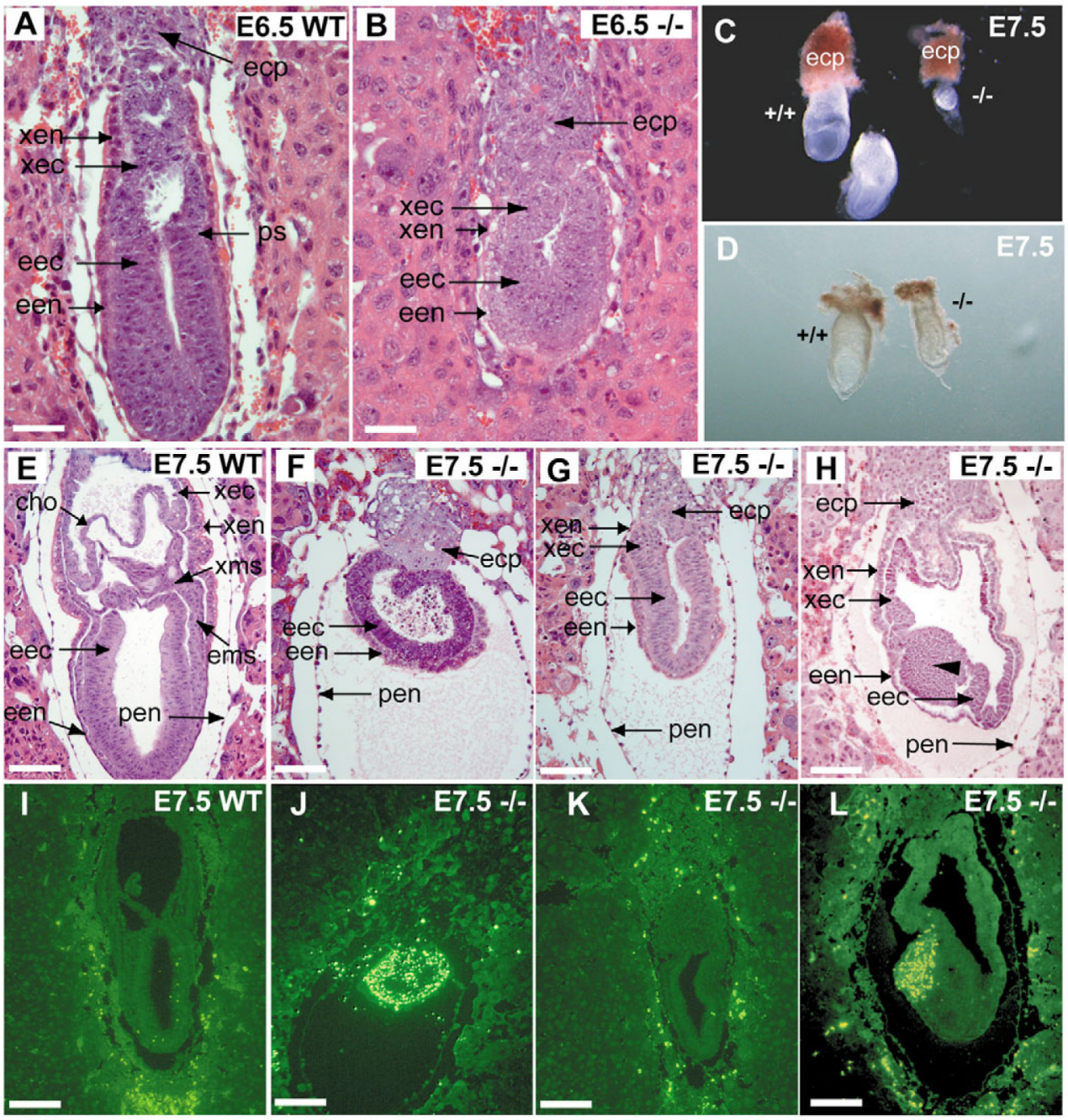

Fig. 2.

Morphological analyses of *Ext2* mutant embryos. In all sections, embryos are viewed laterally and the anterior side of the embryo is towards the left. (A) At E6.5, wild-type embryos have initiated the formation of a primitive streak and show an elongated egg cylinder. (B) $Ext2^{-/-}$ embryos have underdeveloped extra-embryonic structures and do not elongate. There are no signs of primitive streak formation. (C,D) Whole-mount embryos collected at E7.5. (C) Some $Ext2^{-/-}$ mutants show little or no elongation compared with wild-type littermates, but show a normal ectoplacental cone. (D) Other $Ext2^{-/-}$ mutants are only slightly smaller in overall size than wild-type embryos. (E-H) Hematoxylin and Eosin staining of longitudinal sections of wild-type (E) and $Ext2^{-/-}$ (F-H) embryos. (E) At E7.5, a wild-type embryo has well-defined

embryonic and extra-embryonic structures. A layer of mesodermal cells is visible between ectoderm and endoderm. (F) *Ext2*$^{-/-}$ mutant (class 1) with a two-layered, rounded egg cylinder and no visible signs of extra-embryonic ectoderm, endoderm or mesoderm. (G) *Ext2*$^{-/-}$ mutant (class 2) with a two-layered egg cylinder that is about half the size of the wild-type embryo with significantly underdeveloped extra-embryonic structures. (H) A third group of *Ext2*$^{-/-}$ mutants (class 3) shows further elongation of a two-layered egg cylinder. Arrowhead in H indicates the formation of a headfold. (I-L) TUNEL assay examining cell death in wild-type E7.5 embryos (I) and class 1 (J), class 2 (K) and class 3 (L) E7.5 *Ext2*$^{-/-}$ mutants. Little or no cell death is observed in wild type (I) or class 2 *Ext2*$^{-/-}$ mutants (K). The extensive cell death in class 1 mutants shows this embryo is no longer viable (J). Cell death is visible in the headfold of class 3 mutants (L). cho, chorion; ecp, ectoplacental cone; eec, embryonic ectoderm; een, embryonic endoderm; ems, embryonic mesoderm; pen, parietal endoderm (attached to inner aspect of Reichert's membrane); ps, primitive streak; xec, extra-embryonic ectoderm; xen, extra-embryonic endoderm; xms, extra-embryonic mesoderm. Scale bars: 50 μm in A,B; 100 μm in E-H; 140 μm in I-L.

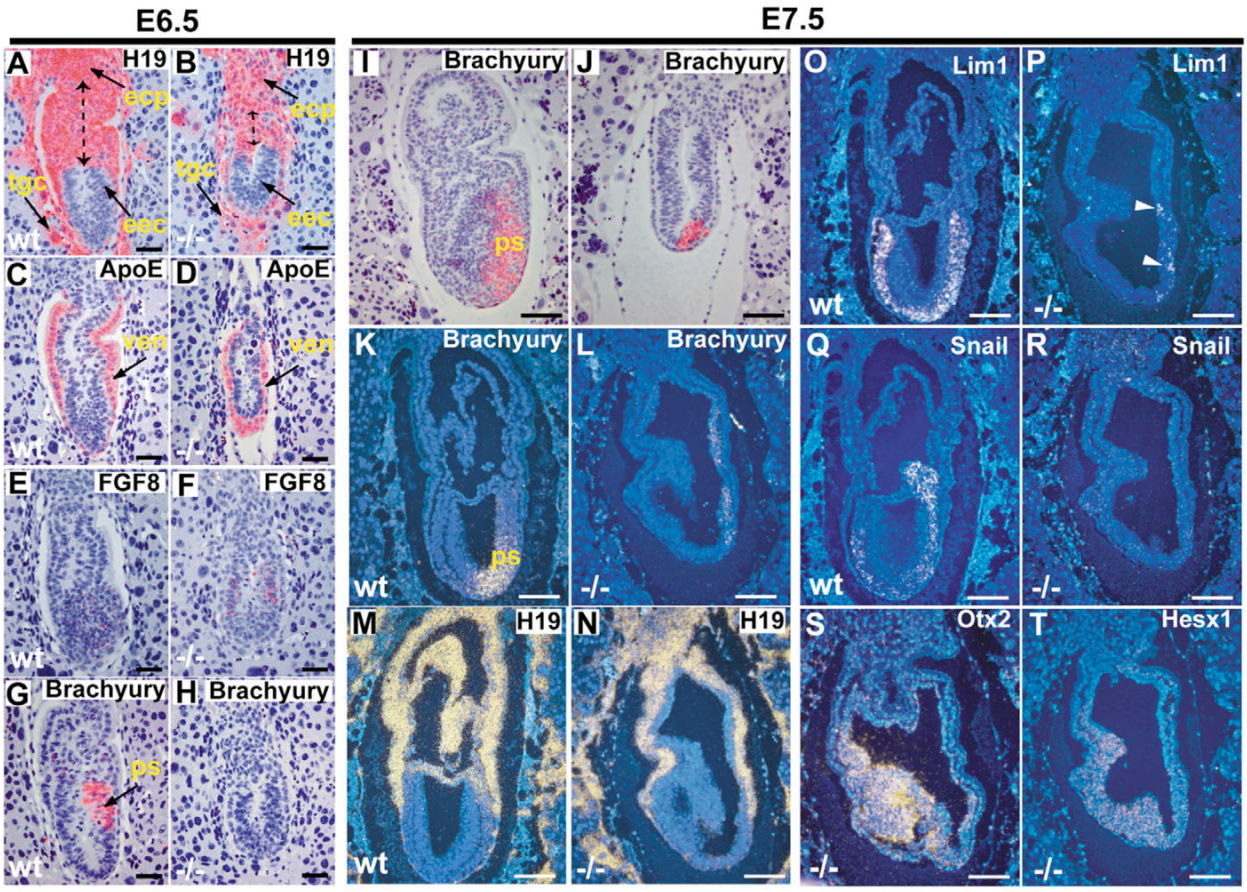

Fig. 3.

In situ hybridization analyses of *Ext2*$^{-/-}$ mutants. Hybridization was performed with ^{35}S-labeled riboprobes and sections were counterstained with Hematoxylin (A-J) or Hoechst (K-T). In all sections, embryos are viewed laterally and the anterior side of the embryo is towards the left. (A-H) Embryos collected at E6.5. (A,B) H19, a marker for extra-embryonic tissues shows the presence of extra-embryonic ectoderm, endoderm, ectoplacental cone and trophoblast giant cells in *Ext2*$^{-/-}$. The broken line indicates the difference in development of the extra-embryonic parts of the egg cylinder. (C,D) Apoe, a marker for visceral endoderm, is expressed in *Ext2*$^{-/-}$ embryos. (E,F) Fgf8, a marker for primitive streak formation, is detected in wild-type embryos and in *Ext2*$^{-/-}$. (G,H) Brachyury (T), another marker for primitive streak and mesodermal cells, is present in wild-type embryos, but not in Ext2 mutants. Embryos collected at E7.5 (I-T). (J) Class 2 mutant; (L,N,P,R,S,T) class 3 mutants; (I,K,M,O,Q) wild type. Brachyury is expressed in class 2 mutants (J) and in class 3 mutants (L,N,P,R,S,T). (M,N) H19 was used as a probe to show the boundaries between embryonic and extra-embryonic regions of the wild-type embryos and *Ext2*$^{-/-}$ mutants. (O,P) *Lim1* is expressed in wild-type embryos at low levels in primitive streak and at higher levels in mesodermal cells migrating away from the streak. Arrowheads indicate several cells expressing Lim1 in the *Ext2*$^{-/-}$ mutants. (Q,R) *Snai1* expression is shown in the primitive streak and nascent mesoderm of wild-type embryos (Q) but is absent in *Ext2*$^{-/-}$ embryos (R). (S) *Otx2* and (T) *Hesx1* mRNAs are detected in the anterior cell mass of class 3 *Ext2* mutants. ecp, ectoplacental cone; eec, embryonic ectoderm; ps, primitive streak; tgc, trophoblast giant cells; ven, visceral endoderm. Scale bars: 50 μm in A-H; 100 μm in I-T.

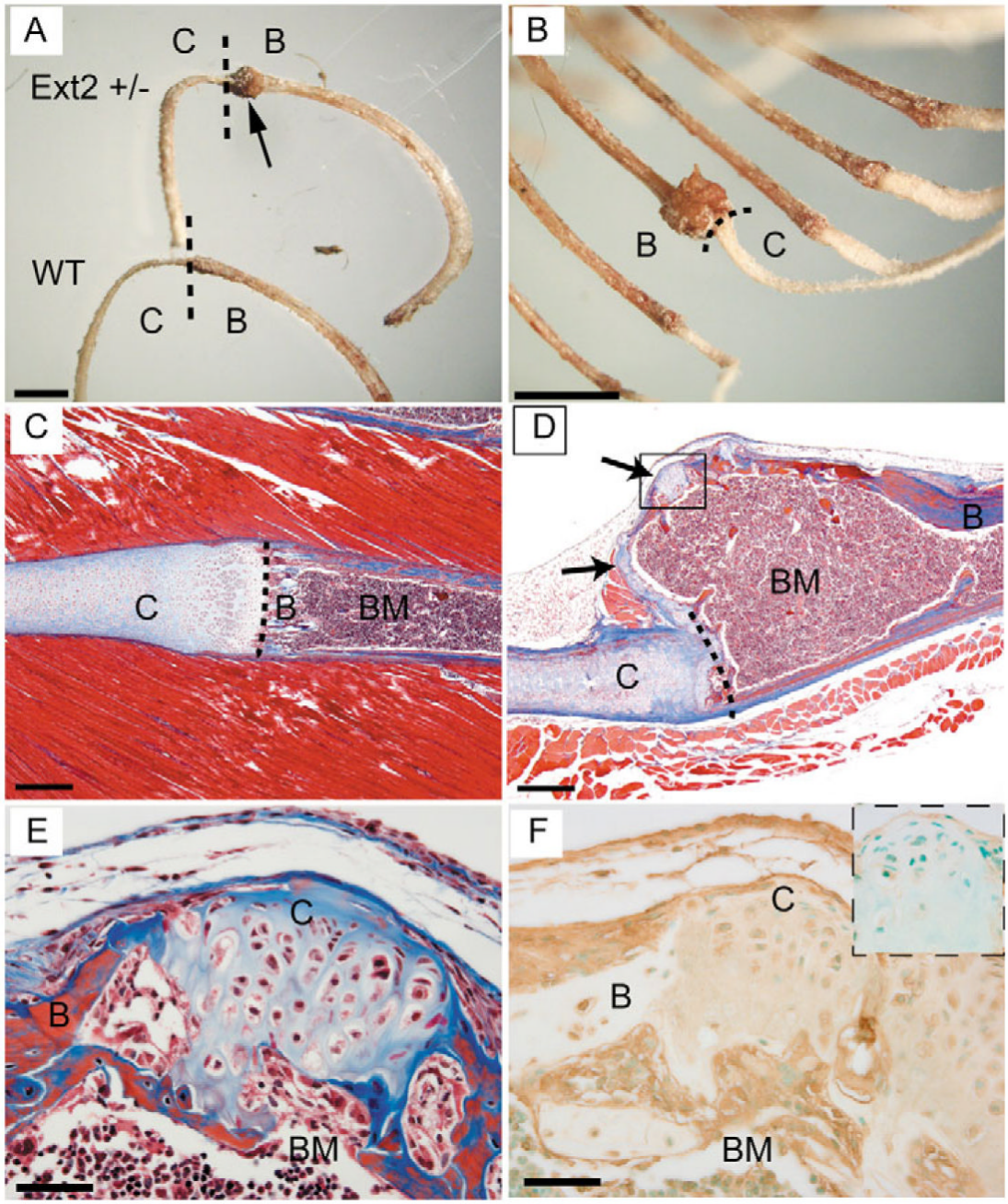

Fig. 4.

Exostosis formation in ribs of *Ext2*$^{+/-}$ mice. (A) Dissected rib of a wild-type mouse and an *Ext2*$^{+/-}$ mouse with an exostosis (indicated by the arrow). The boundaries between the costochondral cartilage and the bony part of the rib are indicated by the broken lines. (B) Higher magnification showing larger exostosis on a rib of an *Ext2*$^{+/-}$ mouse. (C,D) Trichrome-stained histological section of the costochondral junction of rib from a wild-type mouse (C) and a rib from an *Ext2*$^{+/-}$ mouse with an exostosis (D). The exostosis is composed of cortical and medullary bone with an overlying hyaline cartilage cap (indicated by arrows). The bone marrow cavity of the exostosis is continuous with that of the underlying bone. (E) Magnification of the boxed area in D. Within the cartilage cap, some chondrocytes appear to line up, resembling

the organization of chondrocytes in a normal growth plate. (F) Staining of adjacent section to the one shown in E with the HS antibody 10E4 shows that chondrocytes produce HS. Inset in upper right-hand corner shows control staining with mouse IgG as primary antibody. B, bone; BM, bone marrow; C, cartilage. Scale bars: 3.5 mm in A,B; 300 μm in C,D; 50 μm in E,F.

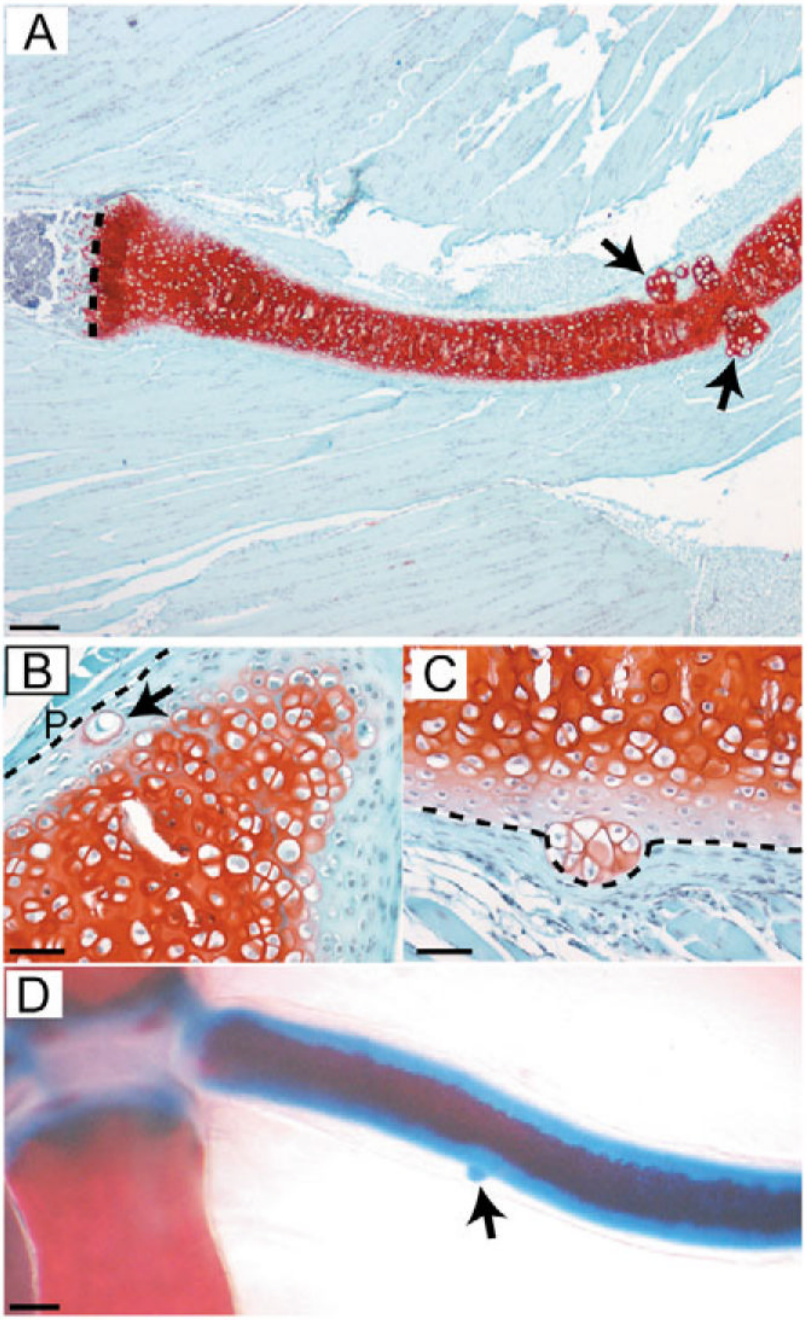

Fig. 5.

Chondrocyte abnormalities. All histological sections have been stained with Safranin O. (A) Longitudinal section of a rib of an *Ext2*$^{+/-}$ mouse shows nodules of displaced chondrocytes (arrows). The costochondral boundary is indicated by a broken line. (B) Transverse section through rib showing single displaced chondrocyte (arrow) near the perichondrium (P). (C) Higher magnification of longitudinal section through a rib of an *Ext2*$^{+/-}$ mouse showing a nodule, forcing the perichondrium to bulge out. In B and C, the broken lines indicate the boundary between perichondrium and cartilage. (D) Low magnification of Alcian Blue (cartilage) and Alizarin Red (bone) staining of a rib of an *Ext2*$^{+/-}$ showing a large nodule (arrow). Scale bars: 200 μm in A; 50 μm in B,C; 300 μm in D.

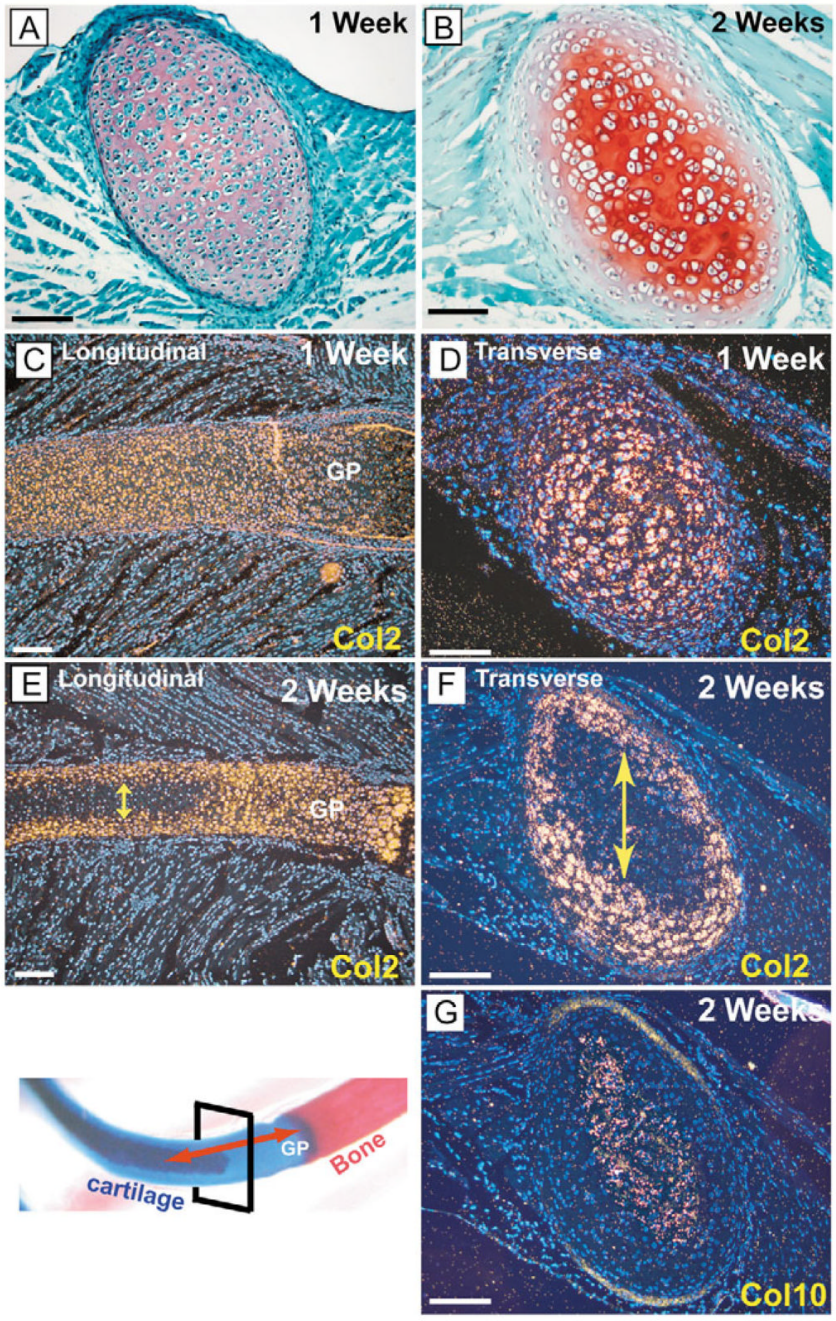

Fig. 6.

Rib cartilage differentiation in wild-type mice. Orientation and location of the sections in this figure are indicated in the bottom left-hand panel of the figure (black rectangle represents transverse section, red arrow represents longitudinal section). (A,B) Transverse sections through the rib cartilage stained with Safranin O. (A) Section through rib of 1-week-old mouse. Chondrocytes have a uniform undifferentiated appearance. (B) Beyond 2 weeks of age, chondrocytes in the center of the element become hypertrophic, while cells in the periphery remain undifferentiated. (C-G) In situ hybridization with probes for Col2 and Col10. (C,D) Until 1 week of age, all chondrocytes, except for the hypertrophic chondrocytes of the growth plate, express Col2. (E-G) At 2 weeks of age, chondrocytes in the center of the rib cartilage

turn off expression of Col2 (area indicated by yellow arrows in E and F), while cells in the periphery, near the perichondrium, continue to express Col2. Chondrocytes in the center now express Col10 (G). GP, growth plate. Scale bars: 100 μm.

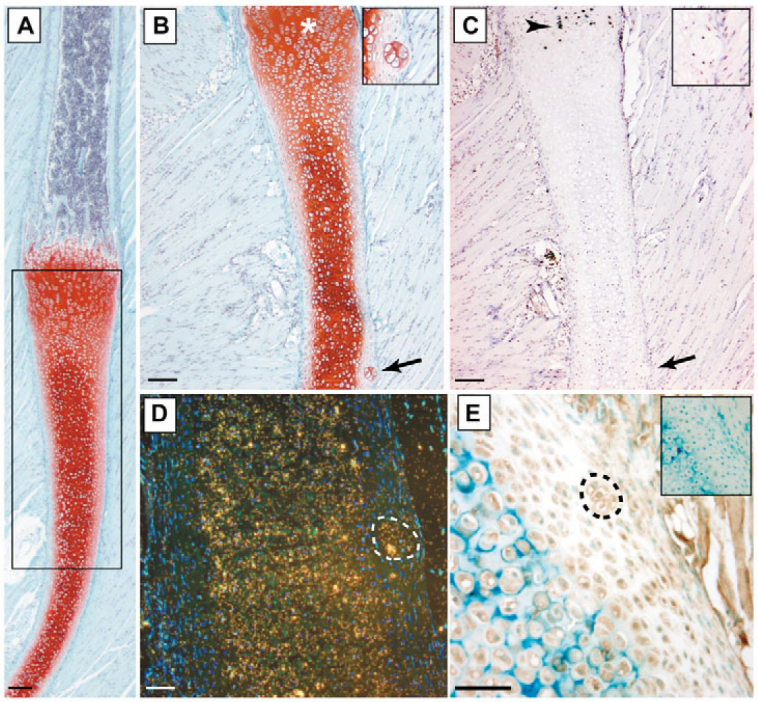

Fig. 7.

(A) Safranin O stained longitudinal section of a rib of a 2-week-old wild-type mouse is shown. Rectangle indicates area of interest representative for B and C. (B) Rib of a *Ext2*$^{+/-}$. Arrow indicates the location of a chondrocyte nodule. Asterisk indicates location of the proliferative zone of the rib growth plate. The inset in the top right-hand corner shows a magnification of the nodule. (C) BrdU staining of adjacent serial section shown in B. BrdU-positive cells can be seen in the proliferative zone of the growth plate of the ribs (arrowhead). The chondrocyte nodule does not contain BrdU-positive cells (arrow). (D,E) Higher magnification of the area with the nodules shown in B and C. (D) In situ hybridization with Col10 antisense probe shows expression by chondrocytes located in the center of the rib cartilage. The nodule of displaced chondrocytes (encircled by the broken line) expresses Col10 and are separated from the centrally located hypertrophic cells by a layer of chondrocytes that do not express Col10. (E) Staining with the HS antibody 10E4 shows that the chondrocytes in the nodules (encircled by the broken line) produce HS. Inset in E shows staining with 10E4 after heparinase treatment. Scale bars: 200 μm in A-C; 50 μm in D,E.

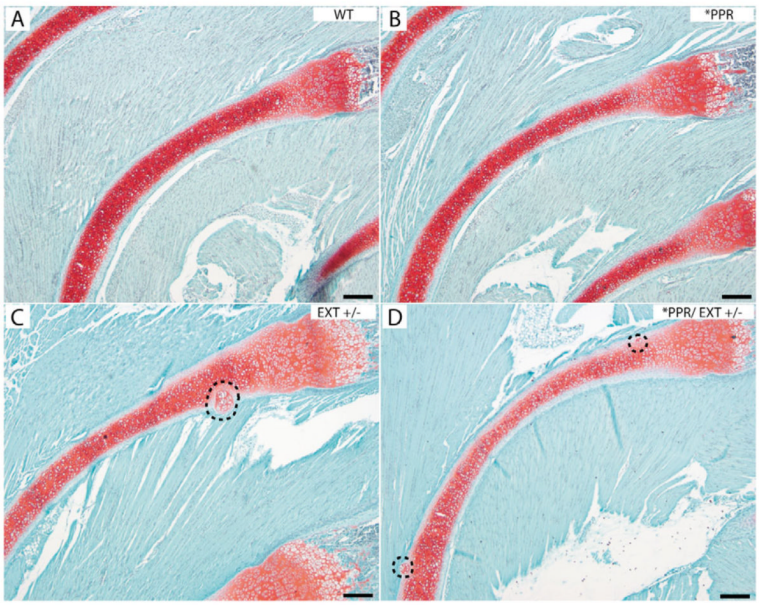

Fig. 8.

A constitutively active Col2-Pthr1 transgene (*PPR) was crossed into the *Ext2*$^{+/-}$ mice. Ribs of wild-type mice (A) and mice carrying the *PPR transgene (B) do not show any cartilage abnormalities. (C) *Ext2*$^{+/-}$ mice show the characteristic nodules (encircled by the broken line). (D) Introduction of the *PPR transgene does not eliminate the premature hypertrophic differentiation in the rib cartilage of *Ext2*$^{+/-}$ mice. Broken lines encircle the nodules. Scale bars: 200 μm.

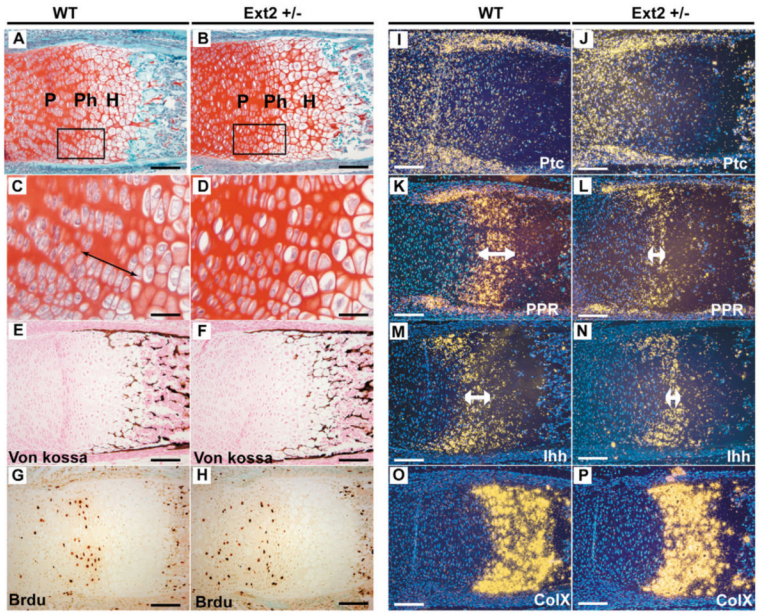

Fig. 9.

Examination of the *Ext2*$^{+/-}$ long bone growth plate. Growth plates from ulnae of E18.5 wild type and *Ext2*$^{+/-}$ were analyzed for proliferation and differentiation defects. (A,B) Safranin O staining shows a similar overall structure of the growth plates of a wild-type and *Ext2*$^{+/-}$ mice. (C,D) Magnification of the rectangular areas in A and B, respectively. Close examination of the chondrocytes in the proliferative zone shows a loss of the characteristic columnar organization normally seen in wild-type growth plates (arrow indicates typical columnar organization). (E,F) Von Kossa stained sections shows the presence of mineralized tissue in the growth plates of both genotypes. (G,H) BrdU labeling shows a similar number of labeled cells in the proliferating zone of the growth plates of wild-type and *Ext2*$^{+/-}$ mice. (I-P) In situ hybridization with markers for chondrocyte differentiation show *Ext2*$^{+/-}$ mice expressed Ptch1, Ihh, Pthr1 (PPR) and ColX in appropriate places but there is a small decrease in the expression domain of Pthr1 and Ihh (compare arrow in K with arrow in L, and arrow in M with arrow in N). P, Proliferating chondrocytes; Ph, Pre-hypertrophic chondrocytes; H, Hypertrophic chondrocytes. Scale bars: 100 μm in A,B,E-P; 50 μm in C,D.

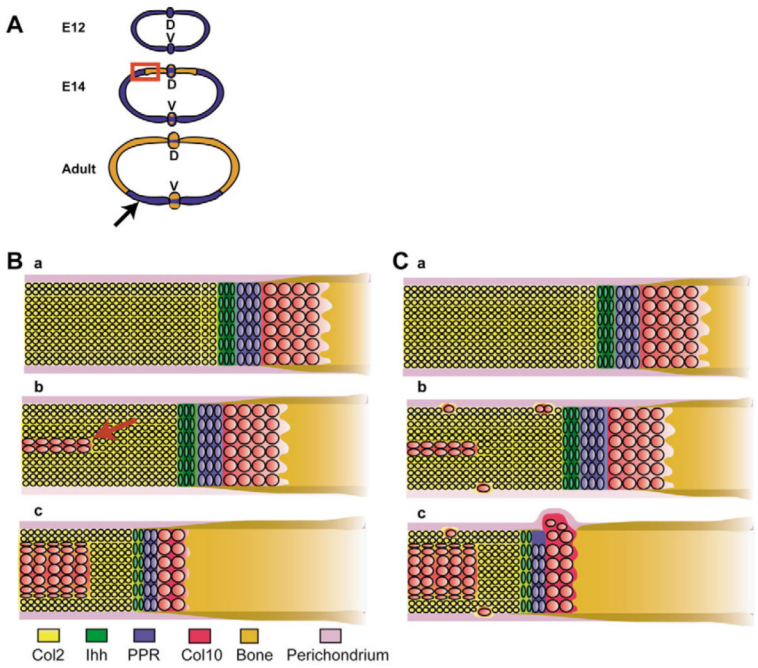

Fig. 10.

(A) Schematic representation of the rib ossification process. At embryonic day 12, the entire rib consists of cartilage. Starting at embryonic day 14, a growth plate is established and ossification begins, proceeding ventrally towards the sternum. The ossification process continues until the mice reach adulthood and an area of permanent costochondral cartilage (arrow) remains throughout life. Red rectangle indicates area represented in B,C. Cartilage is blue and bone is brown. (B) Schematic representation of rib growth plate and chondrocyte differentiation. (a) Around E14, the rib cartilage template becomes invaded by blood vessels, osteoblasts and osteoclasts, and a growth plate is established. Chondrocytes, which are not part of the growth plate, express Col2. (b) When mice reach the age of 2 weeks, chondrocytes in the center of the rib cartilage become hypertrophic and express Col10 (red arrow). (c) When mice reach skeletal maturity, this hypertrophic region expands towards the periphery of the perichondrium, while the growth plate becomes smaller and replacement of cartilage with bone stops. (C) Schematic representation of rib chondrocyte differentiation in Ext2 heterozygotes. (a) During early stages of development, no differences can be observed in between rib cartilage of wild-type and *Ext2*$^{+/-}$ mice. (b) By the age of 2 weeks, however, nodules of Col10-expressing chondrocytes are being formed near the perichondrium as a result of premature hypertrophic differentiation. (c) Formation of an exostosis could be the result of the growth plate moving past a nodule, creating a disruption in bone collar formation. Alternatively, the passage of the growth plate might provide vascularization to the nodule and initiate the bony outgrowth of an exostosis. D, dorsal; V, ventral.

Table 1

Genotype analysis of offspring from $Ext2^{+/-}$ intercrosses

Age	+/+	+/−	−/−	Reabsorbed	Total
E6.5	3 (14%)	12 (57%)	4 (19%)	2 (9%)	21
E7.5	15 (23%)	34 (51%)	14 (21%)	3 (4%)	66
E8.5	8 (15%)	31 (59%)	10 (19%)*	3 (5%)	52
E9.5	8 (26%)	16 (52%)	6 (19%)*	1 (3%)	31
E15.5	10 (38%)	16 (62%)	0	0	26
Neonates	98 (33%)	200 (67%)	0		298

*These were highly abnormal residual embryonic cells that had not yet been resorbed.